AD NUMBER

AD864370

NEW LIMITATION CHANGE

TO

Approved for public release, distribution unlimited

FROM

Distribution authorized to U.S. Gov't. agencies and their contractors; Administrative/Operational Use; 26 NOV 1969. Other requests shall be referred to Army Missile Command, Redstone Arsenal, AL.

AUTHORITY

USAMC ltr, 1 Dec 1972

AD

REPCRT NO. RK-TR-69-15

FEASIBILITY OF ROCKET MOTOR INSULATION INSPECTION USING INFRARED RADIATION
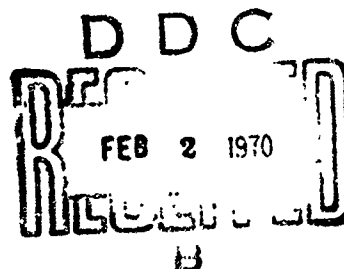
November 1969

by

D. R. Dreitzler
L. B. Thorn

U.S. ARMY MISSILE COMMAND
Redstone Arsenal, Alabama

D D C

FEB 2 1970

B

31

FEASIBILITY OF ROCKET MOTOR INSULATION INSPECTION USING INFRARED RADIATION

by

D. R. Drcitzler
L. B. Thorn

DA Project No. IM262303A205

Measurements Branch
Army Propulsion Laboratory and Center
Research and Engineering Directorate (Provisional)
U. S. Army Missile Command
Redstone Arsenal, Alabama 35809

ABSTRACT

Insulated, thin-wall motor cases have as a potential failure mode the burnthrough of the motor case wall resulting from a defective liner. The objective of this investigation was to determine the feasibility of the use of infrared radiation as a means of non-destructive examination of an insulated motor case in order to detect a potentially defective liner. A relatively inexpensive infrared inspection system was designed and assembled which demonstrated that it is possible to detect cracks and density variations in the insulation of rocket motor cases.

ii

CONTENTS

ILLUSTRATIONS

ABBREVIATIONS

A_D	area of detector
A_s	area of source
cm	centimeter
C_2	constant, 1.432 cm °K
°C	degrees Celsius
°K	degrees Kelvin
d	diameter
dc	direct current
e	Naperian base
H	irradiance
in.	inch
IR	infrared
J	radiant intensity
mm	millimeter
mV	millivolt
mW	milliwatt
N	radiance
n	revolutions per second
NDT	non-destructive t ing
NEP	noise equivalent power
P	pitch
R	responsivity
r	radius
R_c	compensating thermistor
R_t	sensing thermistor
S	distance

iv

ABBREVIATIONS (Concluded)

S_{1N}	distance from 1 to N
S_λ	brightness temperature
t	time, variable
t_r	rise time
t_s	settling time
T	temperature
V	voltage
v	velocity
W_{bb}	energy of blackbody
α_{1N}	angle (deg) from 1 to N
ϵ_λ	emissivity at λ
ϵ_s	emissivity of source
λ	wavelength
μm	micrometer

Section I. INTRODUCTION

Propulsion system requirements for a maximum ratio of payload to initial weight has led to the use of thermally insulated, lightweight, motor cases. These lightweight cases must withstand the extreme temperatures caused by the burning propellant grain without failure. Evidence of motor case failure by burn-through indicates a need for an effective non-destructive inspection technique adaptable to production type quality control procedures. This report describes the feasibility of using IR to measure the variations in heat transfer rate through an unloaded rocket motor case wall and to correlate these measurements with cracking or unbonding of motor case insulation. This technique was selected for evaluation since it would measure directly the variations in thermal conductivity rather than some other parameter from which the heat transfer rate could be inferred. Other techniques include ultrasonic [1] and capacitive [2].

1

Section II. INSTRUMENTATION DESIGN

1. Scanning Technique

Rapid optical scanning of adhesive-bonded flat surfaces using IR-methods resulting in detected surface temperature differences of 0.2°C have been reported [3]. Optical scanning has the advantages of: a) A stationary detector facilitating the use of sensitive cryogenic detectors; b) high scanning speeds resulting from the use of mirrors; c) an easily interpretable output in the form of a thermogram, i.e., a thermal photograph. The main disadvantages of optical scanning for this application are the relatively high cost and the lack of ability to examine both sides of the surface of a cylinder without moving the camera or object. It is noted that a complete thermal map of the surface of a rocket motor case could be obtained during a static firing if two IR cameras with sufficiently short scanning time were available.

A rocket motor case can be examined for surface temperature variations by mechanical movement of the IR detector, the motor case [4], or both. Mechanical scanning was decided upon in this case because of the adaptability of an ordinary machinist's lathe. The lathe is used to rotate the empty motor case at a constant speed while moving the IR sensor parallel to the motor axis near the case surface. The detector thus covers the exterior motor surface by means of a helical path (Figure 1). The pitch of the helix must be chosen to be less than or equal to the diameter, d_i of a resolution element for complete surface coverage. The distance, S, traveled by the detector on the surface of the cylinder during one revolution is approximately given by

$$S^2 = (2\pi r)^2 + P^2 \text{ (meter per revolution)}.$$

In most cases $P^2 \ll (2\pi r)^2$ so that $S = 2\pi r$.

The velocity of the motor case surface with respect to the stationary detector is

$$v = nS = 2\pi rn \text{ (meters per second)} ,$$

where n is in units of revolutions per second. If v is to be maximized for the detector recorder bandwidth available, the rotation rate n must be adjusted for the motor case radius to keep v a constant.

2. Infrared Detector

Choosing a suitable IR detector had to include consideration for its intended use (assembly line NDT of motor cases) as well as for the necessary

2

technical requirements. For simplicity of operation an uncooled detector was considered essential. Anticipated source temperatures at or slightly above 300°K required a wavelength response beyond 9 microns, with a suitable time constant to facilitate rapid scanning. These restraints, coupled with the availability of a type F-S25-S Barnes thermistor, detector, led to its immediate selection. The detector with integral shielded compensating thermistor was used in the voltage divider configuration recommended by the manufacturer [5] (Figure 2).

The detector was mounted inside a solid block of brass with an aperture that limited the field of view to a 60-degree angle. The block was to maintain a stable point of operation by providing a heat sink for the detector mount. This point will be discussed further in the section concerning temperatu   stabilization control of the detector assembly.

An approximation of the expected signal voltage was made by assuming a defect that produces a temperature differential of 1°K on the surface of a heated motor case at 350°K with an emissivity $\epsilon = 0.5$. The radiant power differential emitted by a defect spot of 0.75-cm diameter subtending the detector at a distance (S) of 0.050 in. is given by $\epsilon A_s W_{bb}$, where $W_{bb} = W_{bb}(351°K)$ - $W_{bb}(350°K)$. The irradiance at the detector is calculated from

$$H = \frac{\epsilon A_s}{\pi S^2} W_{bb} \; ,$$

and is equal to approximately 4×10^{-4} watts/cm^2.

The signal voltage V is given by the product of the responsivity R and the total power on the detector according to

$$V = RHA_d \; .$$

By use of the responsivity value of 230 volts per watt specified for the 1-mm^2 detector flake, a signal equal to approximately 1 mV would be expected. This level was considered sufficiently high when compared to the rated noise equivalent power of the thermistor which is calculated to be NEP $\cong 4.2 \times 10^{-10}$ watts. Larger signals will be measured at higher temperatures than 351°K.

3

3. Temperature Stabilization

The thermistor bolometer is designed to exhibit a maximum rate of decrease in resistance with increasing temperature. The thermistor cannot distinguish random ambient temperature variations from those casued by the desired signal radiation. The most commonly used technique to decrease ambient temperature sensitivity is shown in Figure 2. It entails the use of a compensating thermistor, R_c, in series with the sensing thermistor, R_t. Each thermistor flake is designed to be in the same thermal environment except that R_c is shielded from the source radiation to be detected. The output voltage is then dependent on the signal incident on R_t only, assuming the batteries and thermistors are identical. This last situation is not exactly realizable, resulting in some small dc offset as a result of an ambient temperature change. This technique does not stabilize the thermal operating point of the thermistor, thereby causing its responsivity to vary with temperature. This effect along with the output offset problem can be minimized by means of a closed loop temperature control system. The most stable type of controller has been reported [6] to be of the bridge and amplifier type. It has the ability of providing a positive or negative voltage output depending on the direction of the error with respect to the reference temperature. Use of a Peltier type thermo-electric device results in heat being supplied or removed from the controlled device as required. A block diagram of this arrangement is shown in Figure 3. A balancing arrangement is provided as a part of the bias circuit which is of the Wheatstone bridge type. This provides a temperature setting or reference at which the circuit will control. The overall gain, i.e., the product of the pre-amplifier and power amplifier gain, is set at the maximum possible value consistent with stability considerations. If the gain is excessive the system will have excessive overshoot or it will oscillate. An approximate gain value of half the unstable value can be used as a first approximation [7].
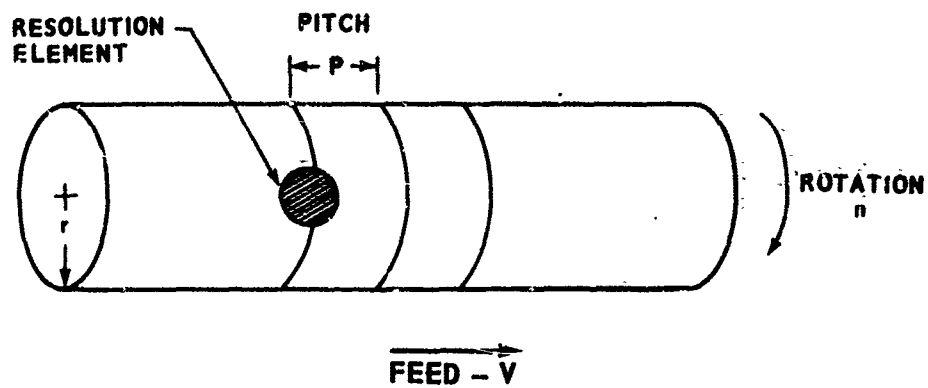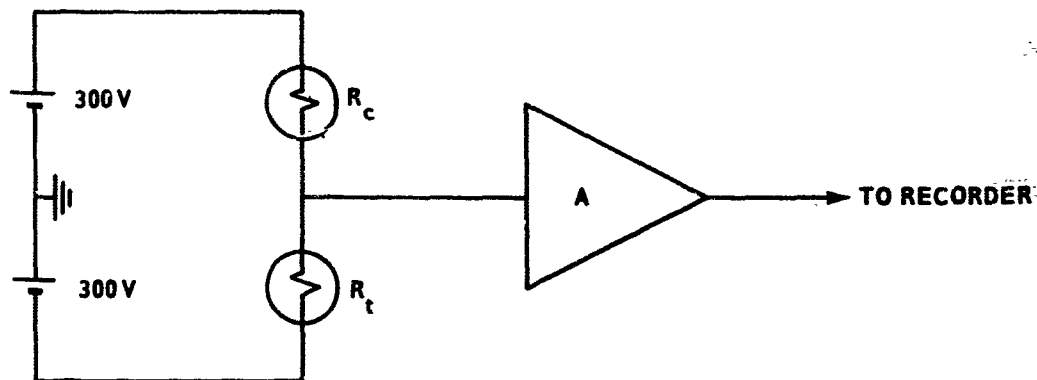
FIGURE 1.   DETECTOR SCAN PATH

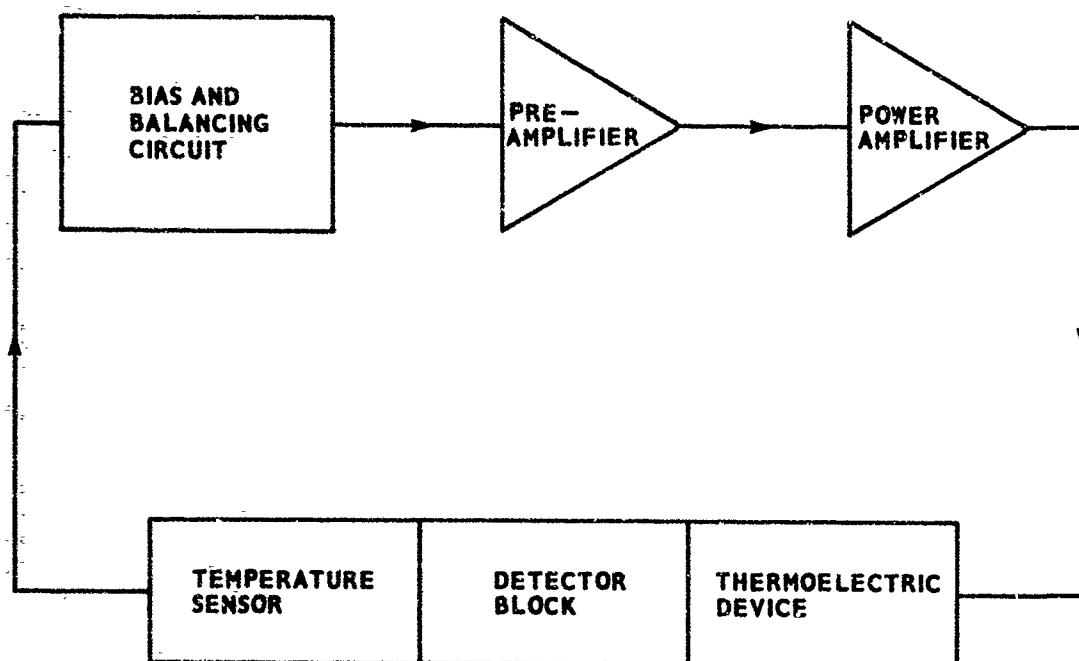FIGURE 2.   THERMISTOR BIAS NETWORK

FIGURE 3.   BLOCK DIAGRAM OF TEMPERATURE
            CONTROLLER

Section III EXPERIMENTAL RESULTS

1. Detector Temperature Stabilization

A wiring diagram of the IR detector temperature controller as used to obtain the results presented in Section III, subsections 2 and 3, is shown in Figure 4. The temperature sensor, R_t, was a 10-kilohm device with a power dissipation constant of 1 mW/°C. Its location in the brass bolometer mounting block was selected with respect to overall symmetry. An electrical connection by means of a shielded cable was made between R_t and the thermistor bias circuit.

This circuit acts to provide a bias voltage to the thermistor so as to transform a variation in the resistance of R_t resulting from changes in the temperature of the brass block to a corresponding voltage. Provision is also made in the bias circuit for eliminating any dc offset in the voltage output. In effect R_2 determines the temperature at which the controller will attempt to maintain the brass block. The output voltage of the bias circuit is amplified to provide sufficient power to the two thermoelectric devices R_{TE1} and R_{TE2} in series so as to return the block to its original temperature. Each of the thermoelectric devices has a heat pumping capacity equivalent to 2 watts at 27°C. Anodized aluminum heat sinks were provided to allow for the heat removal by natural convection.

The stability of the temperature controller was determined by applying a rapid change in temperature to the brass block and observing the closed-loop response of the system. The procedure used to display the temperature stability information is as follows:

a)   A parallel connection to the preamplifier input shown in Figure 4 was made to the Y input of a Mosely 135A X-Y recorder used as a Y-t recorder.

b)   The Y input was then calibrated in terms of temperature.

c) R_2 was adjusted to provide a zero output at 80°F.

d)   The instrument brass block was then placed in a Delta MK 2800 temperature chamber set at 83°F.

e)   The brass block and oven were allowed to reach thermal equilibrium at a temperature of 76°F.

f)   The Delta temperature chamber and the controller were then simultaneously energized and the results recorded as shown in Figure 5. The time domain parameters [8] obtained from Figure 5 are:

7

1) Maximum response = 35 mV

2) Final response = 34 mV

3) Rise time, t_r, = 20 sec

4) 5-percent settling time, t_s, = 100 sec

5) Percent overshoot = 2.9

6) Period of oscillation = 25 sec.

These figures indicate that the control system is relatively stable.

The reduction in drift of the thermistor bolometer was determined by recording the zero drift of the IR detector with the temperature controller on and off. A block diagram of the complete system is shown in Figure 6. With a controller gain of 2000 the bolometer drift was reduced from 8 to 1 mV/sec.

2. Rotating Disk

A number of techniques for appling heat to a test object during IR non-destructive inspection have been investigated [9]. The method selected for use in this feasibility study is that of scan heating with a localized heat source. This approach was selected in order to minimize overall heating of both the detector and object being examined.

A disk was selected as the first object to be examined because of the ease of fabrication and simplicity of scanning. The disk was made by attaching a 0.004-inch thick stainless steel disk to a 6.5-inch diameter plexiglass disk of 0.25-inch thickness with RTV silicone rubber adhesive. In addition, two 0.5-inch holes were drilled in the plastic material equidistant from the disk center a distance of 2 inches located on a diameter.

An automobile type lighter element was selected as the IR heat source because of its small size and high rate of radiant energy transfer. A measurement of the brightness temperature of the lighter element at the power input of 32 watts (8 volts at 4 amperes dc) used in obtaining the results described in this section was made by use of a Leeds and Northrup optical pyrometer. The pyrometer compared favorably with a Barnes Engineering blackbody at 900°C. Assuming a value of emissivity of an oxidized nichrome surface $\left(\epsilon_\lambda = 0.87 \text{ for}\right.$

red light at 0.65 μm$\bigg)$ the true temperature, T, was calculated to be approximately 1180°K by the Wien equation [10]:

$$\frac{1}{T} - \frac{1}{S_\lambda} = \frac{\lambda}{C_2} \frac{\log \epsilon_\lambda}{\log e} \ .$$

The radiating area of the lighter was 1.48 cm^2. By use of the Stefan-Boltzman law for the total radiance, the radiant intensity, $J = NA_s$, of the element becomes 4.41 watts per steradian.

The disk was rotated by a lathe at approximately 0.4 hertz. The following three detector source arrangements were evaluated:

    a)   Source and detector in line on opposite sides of the disk with the stainless steel side heated.

    b)   Source and detector in line on opposite sides of the disk with heat applied to the plexiglass side.

    c)   Source and detector located on the stainless steel side with the source leading the detector by 90 degrees.

The recorded signal levels corresponding to a), b), and c), respectively, were 1.3, 0.2, and 0.7 inches with a recorder sensitivity of 0.5 mV/in. The signal recorded by method a) is shown as Figure 7. The indications numbered 1 and 4 were visually observed to correspond with the passage of the 0.5-inch holes in the plexiglass (Figure 7) past the IR detector. Point 7 is a repeat of point 1.

The maximum signal variations, numbered 2, 3, 5, and 6, can be attributed to gross density variations in the RTV bonding material. The angular displacement of each indication was calculated by means of the relationship:

$$\alpha_{1N} = \frac{S_{1N}}{S_{17}} \times 360° = \frac{360}{4.90} S_{1N} = 73.5 \, S_{1N} \text{ deg,}$$

where

    α_{1N} = angle from point 1 to N (deg)

    S_{1N} = distance from 1 to N obtained from Figure 7 (in.)

    S_{17} = distance of one complete cycle, obtained as shown above (in.)

The values obtained for the points numbered 1 through 7 are listed in Table I along with the minimum deflection occurring between these points. A

TABLE I. ANGULAR DISPLACEMENT OF RECORDED
SIGNAL VARIATIONS FROM POINT 1

Indication No. N	d_{1N} (in.)		α_{1N} (deg)	
	Maxima	Minima	Maxima	Minima
1	0	0.3	0	22
2	1.45	0.8	107	59
3	1.95	1.7	143	125
4	2.45	2.1	180	154
5	3.25	3.06	239	225
6	4.30	3.53	316	260
7	4.90	4.63	360	340

polar plot (Figure 9) of these points is shown at the detector radius super-
imposed on a sketch of the outlines of the density variations observed from the
photograph of Figure 8.

The calculated location of the holes in the plexiglass agrees with their
actual location to within less than 1 percent. The visually observed variations
in the RTV bonding material seen in the photograph (Figure 8) do not exactly
correspond with the location of the maxima and minima plotted in Figure 9.
This might be attributed to the lack of uniformity of the bonding defect.

3. Motor Case Data

The following methods were used to establish the feasibility and
technical problem areas of an IR scanning NDT applicable to detection of rocket
motor defects.

A motor case of $1/16$-inch steel, 3-inch inside diameter by 10-inch length
was insulated with a $1/16$-inch sheet of phenolic asbestos. A small amount of
grease was applied to a localized area of the case to create an unbonded region
during liner attachment to the motor case. The insulation was cut to form a
triangular crack $1/10$ inch at the widest point. The apex decreased to a hairline
approximately $2\frac{1}{2}$ inches from the motor edge and extended the length of the
case (Figure 10). With these "built-in" defects the output signals of the IR
sensor could be more easily interpreted.

A helical scanning technique was used in which the motor was rotated on a lathe spindle while the sensor, mounted on the carriage, traversed the case parallel to its axis.

Various methods were investigated to raise the surface under inspection to a measurable temperature. These methods involved the use of radiant and convective heating of both large and small areas from either inside or outside the motor wall [9]. Spot heating by tungsten lamps resulted in insufficient energy transfer for the required temperature differential. Radiant heating of the interior of the case by an axially mounted heating element rapidly increased the thermistor detector temperature above its optimum operational range. This problem was also experienced during convection heating by hot air. To maintain a small resolution element without resorting to lenses, it was necessary to locate the sensor within a minimum distance of the motor wall of about 0.050 inch. This fact appeared to eliminate all methods involving total heating of the motor case. The most successful approach involved the use of an automobile lighter mounted inside the motor wall with the sensor outside. The lighter provided sufficient radiant energy to produce sensor signals indicative of the radial rate of heat transfer through the motor wall. With the sensor and lighter mounted stationary with respect to each other on the carriage, and on opposite sides of the motor wall, the entire surface could be scanned. An advantage of this heating technique is that the elliptical shape of the motor case does not appreciably affect the signal level. Signal variations due to heating by the inverse square effect are effectively compensated by maintaining a fixed radial distance between the source and sensor, regardless of the wall position. It was found that optimum positioning at the lowest rotation rate of the lathe was when the sensor was displaced 90 degrees with respect to the lighter.

First attempts to identify insulation defects from the recorded signals were unsuccessful. This fact was later attributed to emissivity variations which appeared to predominate over the surface temperature variations. In an effort to eliminate emissivity variations, the motor case was sprayed with a uniform coating of flat black paint and the experiment attempted once more. This time a clear correlation could be drawn between the record and the positions of the defective areas. Figure 11 illustrates successive helical scans of the motor surface. In reference to Figure 10, which is a scale layout of the motor, one may see the beginning point of each scan, located about 5½ inches from the right end.

With the lateral scan rate of 0.11 inch per second and a motor rotation rate of 0.4 revolution per second, the total scan time for the inspected area was approximately 50 seconds. The exact size of the unbonded area was unknown, and it is therefore difficult to establish with certainty that the scans reflect its existence; however, irregularities measured while the sensor was in the area

of the unbond seem to indicate its detection. The regularity of the recorded pulses in the area of the crack leaves no doubts whatever concerning its detection. The intensity and duration of the pulse in the widening area of the crack are clearly observed. Extrapolation of the pulse interval to the beginning of the trace also reveals a slight indication of the hairline crack along the full length of the case. From these considerations and results found in the current literature [4] it is possible to conclude that IR inspection of motor cases is definitely feasible.
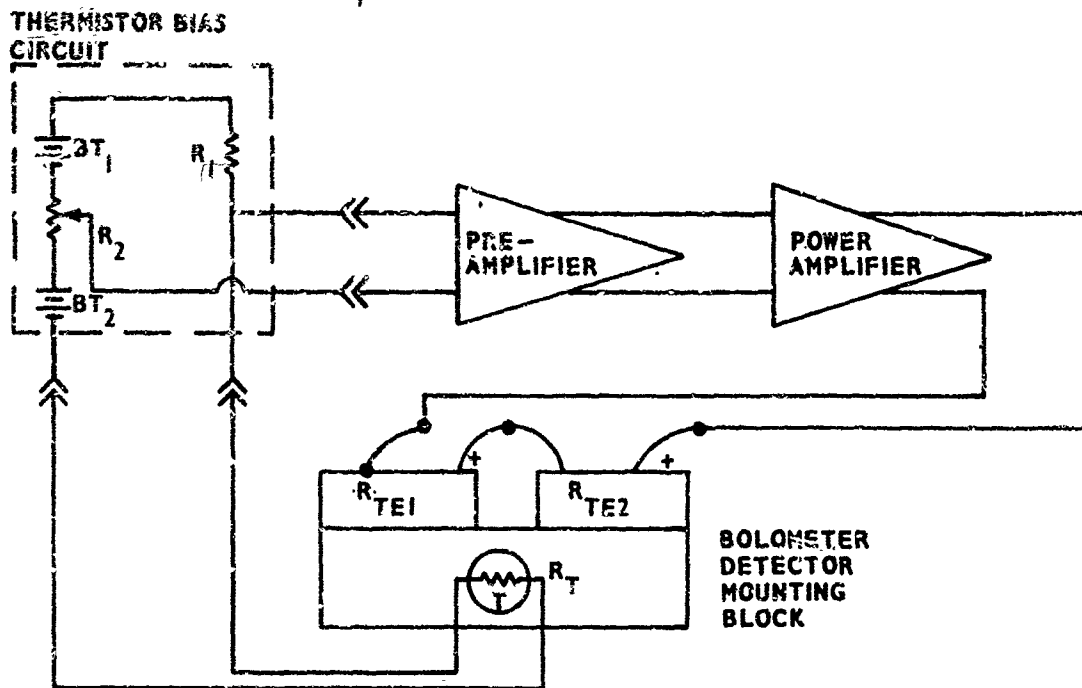
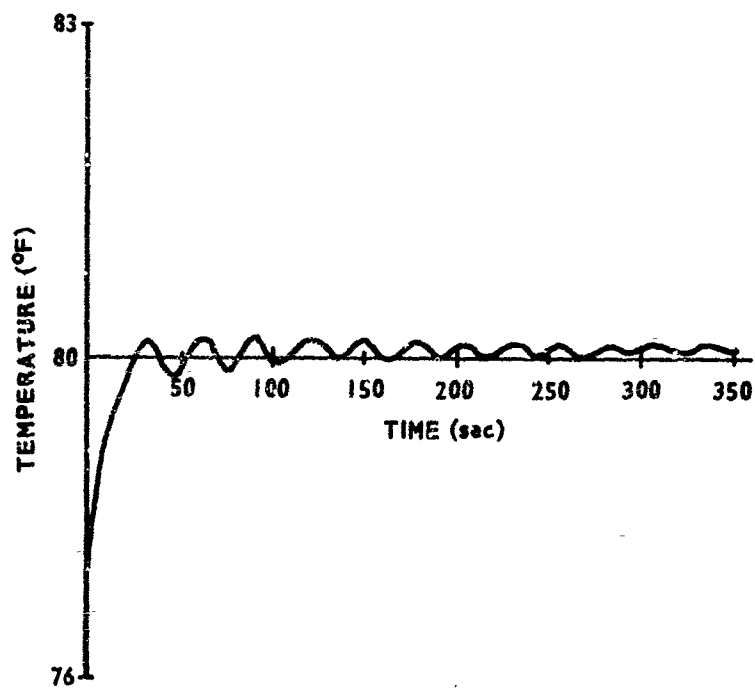FIGURE 4.   WIRING DIAGRAM OF TEMPERATURE CONTROLLER
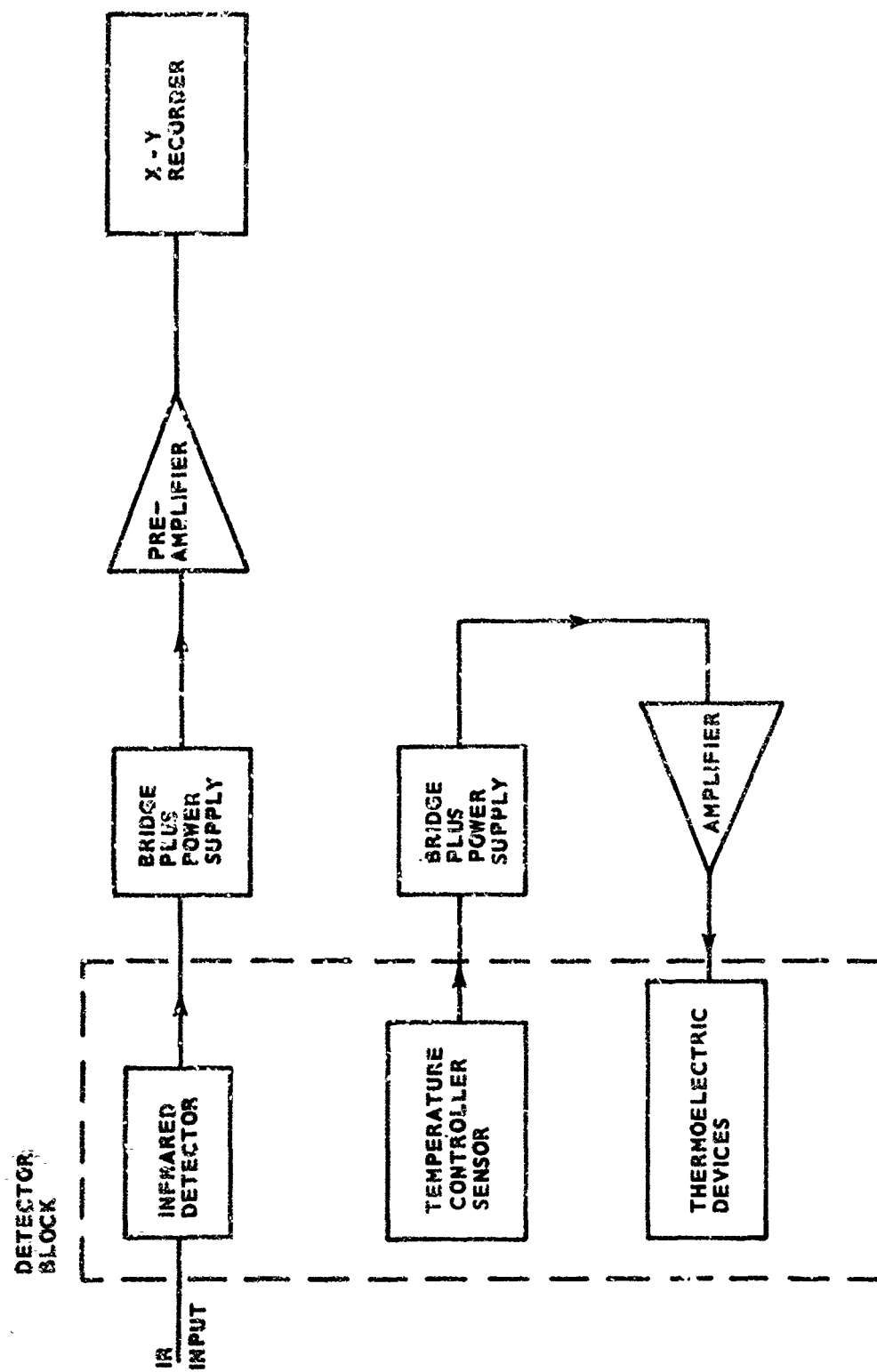

FIGURE 5.   CONTROLLER STEP RESPONSE
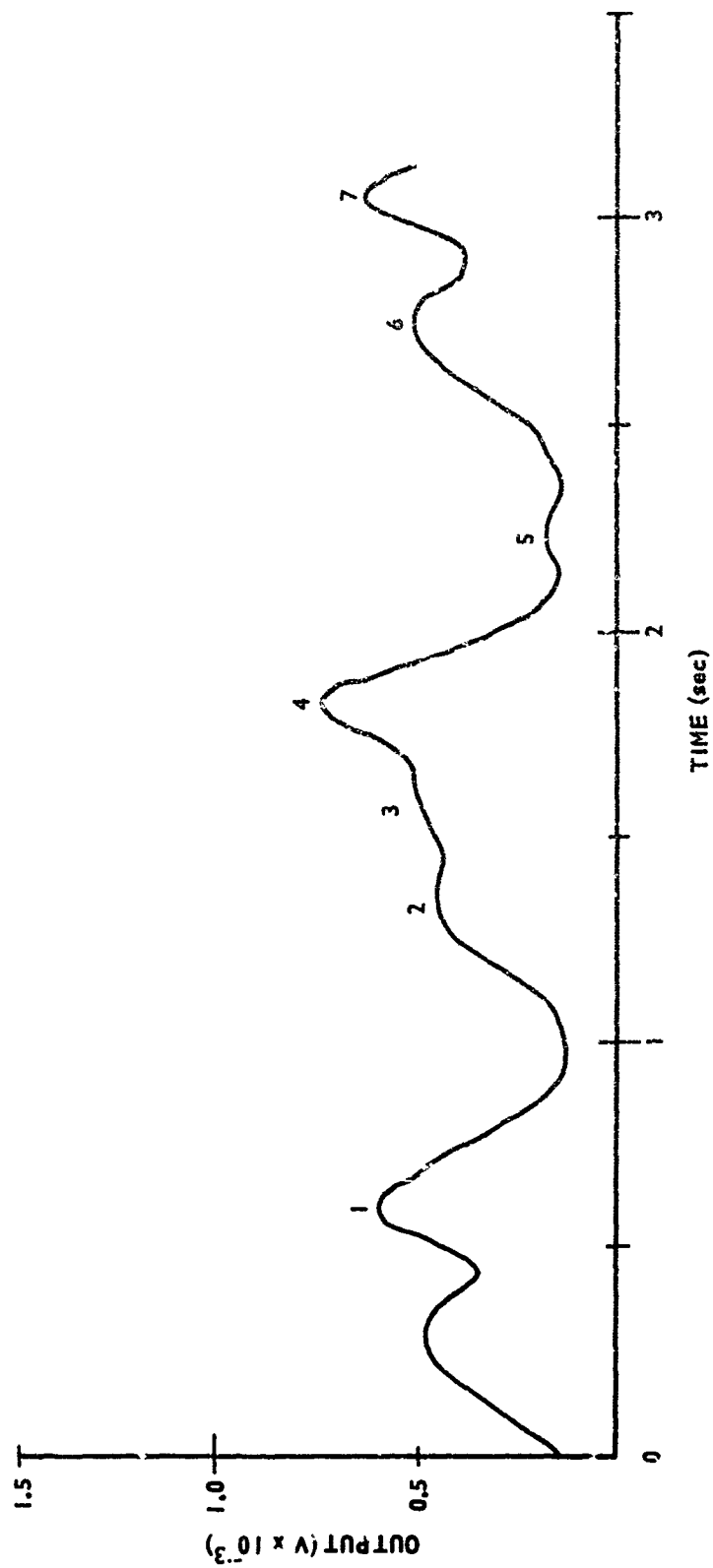
FIGURE 6. OVERALL BLOCK DIAGRAM

14

FIGURE 7. DISK SCAN, INSULATED SIDE HEATED

15
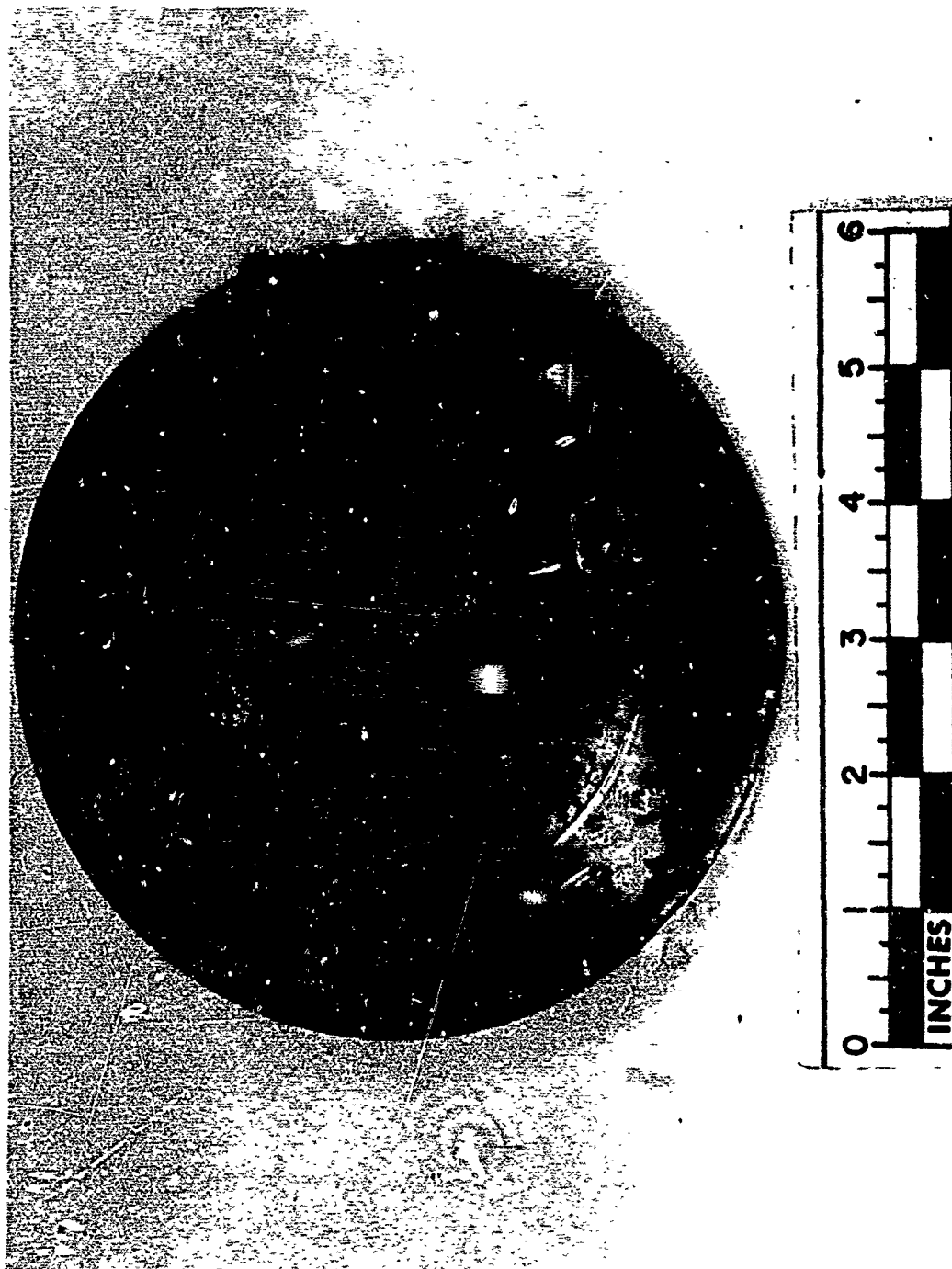
FIGURE 8. PHOTOGRAPH OF INSULATED DISK
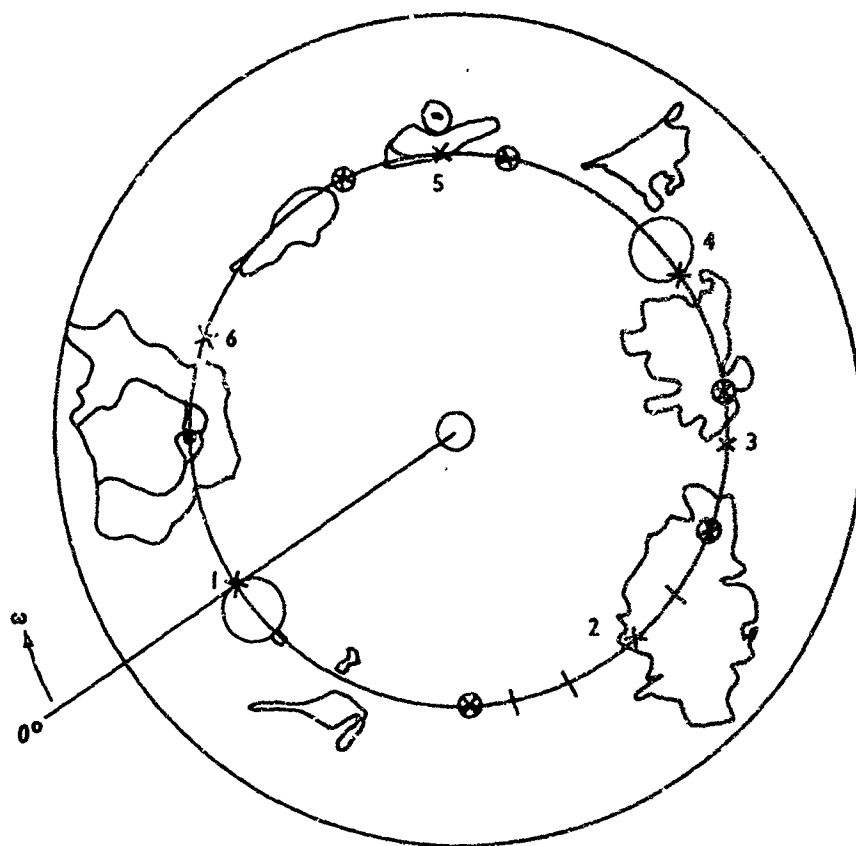
16

X - MAXIMA
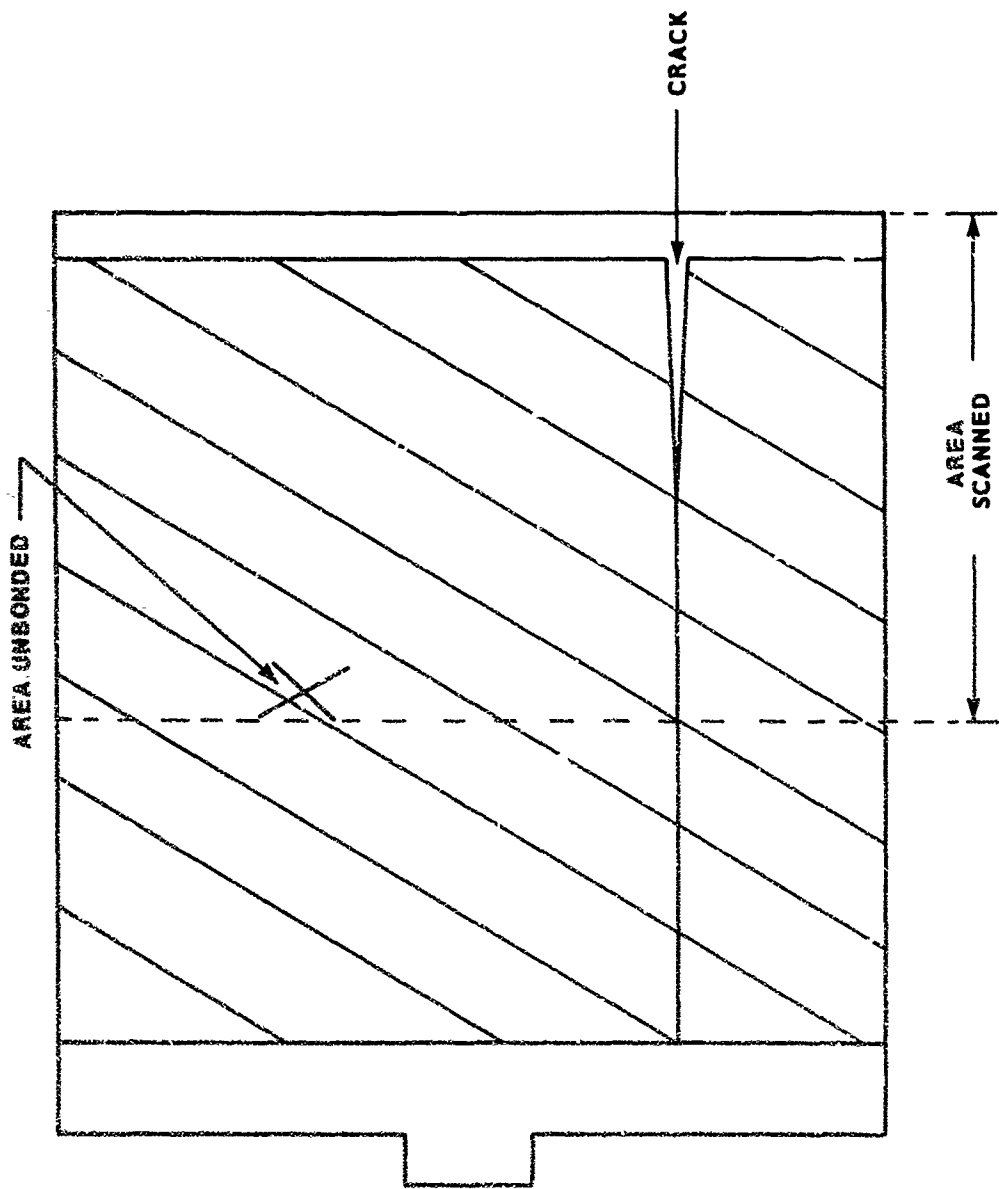
⊗ - MINIMA

FIGURE 9. POLAR PLOT OF DETECTOR RESPONSE

17

CRACK

AREA SCANNED

AREA UNBONDED

FIGURE 10. DEVELOPMENT OF DEFECTIVE MOTOR CASE

18

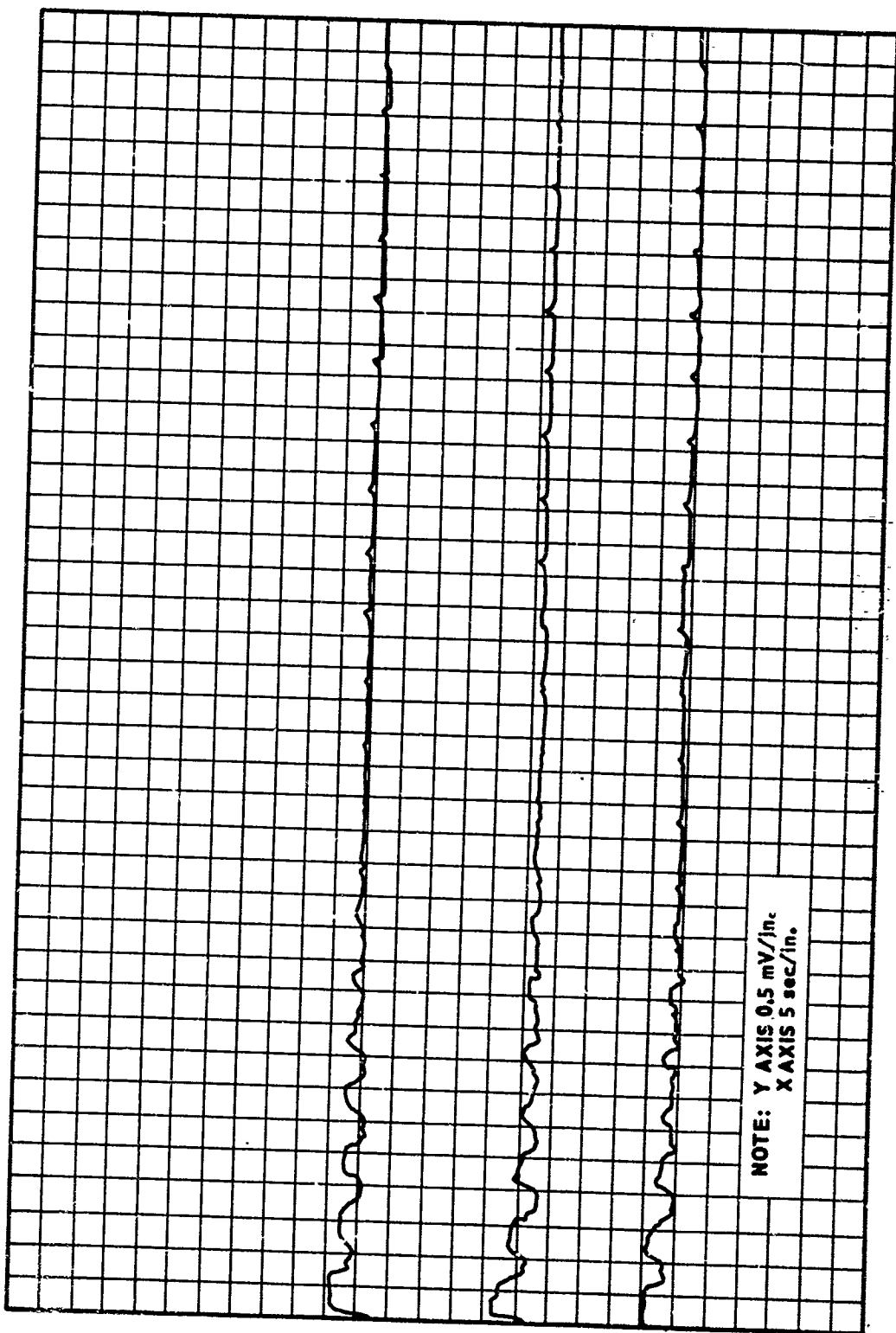NOTE: Y AXIS 0.5 mV/inc
X AXIS 5 sec/in.

FIGURE 11. SUCCESSIVE SCANS OF DEFECTIVE MOTOR CASE

19

Section IV. CONCLUSIONS AND FUTURE PLANS

From this study it has been determined that: 1) It is feasible to use IR radiation as a means of non-destructive testing of rocket motor case insulation; 2) The non-cryogenic thermistor bolometer has sufficient sensitivity to detect insulation non-uniformities; 3) A closed loop control system is useful to stabilize the detectors' thermal operating point, permitting dc coupling of the detector output.

Future work will involve optimizing individual component performance in order to increase the overall system response. Germanium immersed thermistor detectors with appropriate preamplifiers will be mounted in a thermoelectrically stabilized assembly operated near room temperature. A recording technique will be selected to ease data interpretation. An example would be to intensity-modulate a storage oscilloscope in order to produce a thermal image similar to a photograph of the motor case being inspected. The system bandwidth must be sufficient to allow detection of predicted defects at the selected scanning speed.

The system obtained as a result of the above procedure will be used to examine a number of motor cases with known insulation defects. These motor cases will then be static fired in order to correlate the inspection results with actual motor case failures such as case burnthrough. Instrumentation to detect localized motor case heating while static firing will be evaluated, e.g., the Barnes IR camera, if a unit becomes available.

REFERENCES

1. U. S. Army Missile Command, Redstone Arsenal, Alabama, Redeye Rocket Motor Case Insulation Bond Investigation by Otis D. Hartley, November 1968, Report No. RT-TM-69-2.

2. Lion, K. S., Instrumentation in Scientific Research, McGraw-Hill Book Company, New York, 1959, p. 166.

3. Kutzcher, E. W., Zimmerman, K. H., and Botkin, J. L., "Thermal and Infrared Methods for Nondestructive Testing of Adhesive Bonded Structures," Transactions of Infrared and Thermal Sessions of American Society for Non-Desctructive Testing, Inc., October 1967, p. 52.

4. Vogel, P. E., "Evaluation of Bonds in Armour Plate and Other Materials Using Infrared Non-Desctructive Testing Techniques," Applied Optics, Vol. 7, No. 9, September 1968, pp. 1739-1742.

5. Barnes Engineering Company, Bulletin No. 2-100, Thermistor Infrared Detectors.

6. Gheorghiu, Paul, "Contribution to the Fast Warm-up and Close Temperature Control Oven Theory," IEEE Transactions on Industrial Electronics and Control Instrumentation, Vol. IECI-13, April 1966, p. 86.

7. Caldwell, W. I., Coon, G. A., and Zoss, L. M., Frequency Response for Process Control, McGraw-Hill Book Company, New York, 1959, p. 32.

8. Melsa, J. L., and Schultz, D. G., Linear Control Systems, McGraw-Hill Book Company, New York, 1969, p. 378.

9. Maley, D. R., "Two Thermal Nondestructive Testing Techniques," Transactions of the Infrared Sessions, February 1965, Paper No. 4.

10. Forsythe, W. E., Measurement of Radiant Energy, McGraw-Hill Book Company, New York, 1937, p. 380

DOCUMENT CONTROL DATA - R & D

(Security classification of title, body of abstract and indexing annotation must be entered when the overall report is classified)

1. ORIGINATING ACTIVITY *(Corporate author)*	2a. REPORT SECURITY CLASSIFICATION
Army Propulsion Laboratory and Center Research and Engineering Directorate (Provisional) U. S. Army Missile Command Redstone Arsenal, Alabama 35809	Unclassified
	2b. GROUP N/A

3. REPORT TITLE

FEASIBILITY OF ROCKET MOTOR INSULATION
INSPECTION USING INFRARED RADIATION

4. DESCRIPTIVE NOTES *(Type of report and inclusive dates)*

None

5. AUTHOR(S) *(First name, middle initial, last name)*

D. R. Dreitzler
L. B. Thorn

6. REPORT DATE	7a. TOTAL NO. OF PAGES	7b. NO. OF REFS
26 November 1969	27	10

8a. CONTRACT OR GRANT NO.	9a. ORIGINATOR'S REPORT NUMBER(S)
b. PROJECT NO. (DA) 1M262303A205	RK-TR-69-15
c. AMC Management Structure Code No.	9b. OTHER REPORT NO(S) *(Any other numbers that may be assigned this report)*
d.	AD

10. DISTRIBUTION STATEMENT

This document is subject to special export controls and each transmittal to foreign governments
or foreign nationals may be made only with prior approval of this Command, ATTN:
AMSMI-RK.

11. SUPPLEMENTARY NOTES	12. SPONSORING MILITARY ACTIVITY
None	Same as No. 1

13. ABSTRACT

Insulated, thin-wall motor cases have as a potential failure mode the burnthrough
of the motor case wall resulting from a defective liner. The objective of this
investigation was to determine the feasibility of the use of infrared radiation as a means
of non-destructive examination of an insulated motor case in order to detect a potentially
defective liner. A relatively inexpensive infrared inspection system was designed and
assembled which demonstrated that it is possible to detect cracks and density variations
in the insulation of rocket motor cases.

DD FORM 1473 REPLACES DD FORM 1473, 1 JAN 64, WHICH
OBSOLETE FOR ARMY USE.

Security Classification

14. KEY WORDS	LINK A		LINK B		LINK C	
	ROLE	WT	ROLE	WT	ROLE	WT
Insulated motor case Non-destructive examination Infrared radiation						